26 eV yields reactions 22-25. As is expected from the above

$$FeC_{10}H_{10}^{+} \xrightarrow{26\ eV} Fe^{+} + C_{10}H_{10} \quad 38\% \quad (22)$$

$$\longrightarrow C_{10}H_{8}^{+} + FeH_2\ (\text{or } Fe + H_2) \quad 12\% \quad (23)$$

$$\longrightarrow FeC_8H_8^{+} + C_2H_2 \quad 11\% \quad (24)$$

$$\longrightarrow FeC_{10}H_8^{+} + H_2 \quad 39\% \quad (25)$$

discussion of the mechanism, a wide variety of isomeric product ions should be possible. While the large numbers of possible isomers make the study of the CID reactions for each one of them more difficult, the general mechanisms outlined above should be useful in predicting the most likely isomers present.

Conclusion

Interesting reactivity is observed for Fe^+-benzyne. Fe^+ can induce polymerization of chlorobenzene to form Fe^+-polyphenylene or C-C inserted polyphenylene via dehydrochlorination up to the sixth step. The reaction to form Fe^+-hexaphenylene is significantly slower than the earlier steps. Collision-induced dissociation on Fe^+-polyphenylene suggests that bisphenylene, trisphenylene, and tetraphenylene all have ionization potentials lower than that of Fe at 7.870 eV.

The observed reactions between Fe^+-benzyne and alkanes suggest that Fe^+ acts as the reaction initiation center in Fe^+-benzyne. All reactions between Fe^+-benzyne and alkanes can be explained by initial Fe^+ insertion into a C-H or C-C bond, followed by migration of an alkyl or H onto the benzyne ligand or, alternatively, by benzyne migratory insertion into a Fe^+-H or Fe^+-alkyl bond. Fe^+-benzyne reacts with all of the alkanes studied, with the exception of methane. With the exception of ethane, all of the alkanes studied having 1,2-hydrogen atoms hydrogenate benzyne to form Fe^+-benzene. CID study suggests formation of Fe^+-benzocyclobutene from ethane, which is favored over the hydrogenation product ion. However, the isomeric ion Fe^+-styrene is formed from reactions with propane, *n*-pentane, and *n*-hexane. The ion with the formulation of $FeC_9H_{10}^+$ produced from propane and isobutane consists of at least two isomeric forms, Fe^+-α-methylstyrene, Fe^+-3-phenylpropene, and/or Fe^+-β-methylstyrene. However, for the ion of the same formulation generated from *n*-butane, the CID results clearly indicate the absence of Fe^+-α-methylstyrene. All of these results can be explained by a series of mechanisms based on Fe^+ acting as the reaction center.

Acknowledgment is made to the Division of Chemical Sciences in the Office of Basic Energy Sciences in the U.S. Department of Energy (DE-FG02-87ER13766) for supporting this research and to the National Science Foundation (CHE-8612234) for continued support of the FTMS.

Registry No. VIII, 119208-10-5; XIII, 119208-11-6; $FeC_6H_4^+$, 119208-09-2; $FeC_6H_6^+$, 102307-51-7; chlorobenzene, 108-90-7; methane, 74-82-8; ethane, 74-84-0; propane, 74-98-6; *n*-butane, 106-97-8; *n*-pentane, 109-66-0; *n*-hexane, 110-54-3; isobutane, 75-28-5; neopentane, 463-82-1; styrene, 100-42-5; ethylbenzene, 100-41-4; *o*-xylene, 95-47-6.

Investigations of Small Carbon Cluster Ion Structures by Reactions with HCN

Denise C. Parent* and Stephen W. McElvany

Contribution from the Chemistry Division/Code 6110, Naval Research Laboratory, Washington, D.C. 20375-5000. *Received September 12, 1988*

Abstract: The results of a detailed study of the primary and secondary reactions of carbon cluster ions, C_n^+ ($3 \le n \le 20$), with HCN are used as a probe of the structures of small carbon cluster ions. The experiments were performed in a Fourier transform ICR mass spectrometer (FTMS), using direct laser vaporization of graphite to form the carbon cluster ions. The only ionic products observed for the HCN reactions were C_nX^+ (primary reaction product) and C_nXY^+ (secondary reaction product) where X and Y = H, CN, or HCN. Radiative association is an important reaction channel. Products resulting from fragmentation of the reactant carbon cluster ion were not observed. Evidence for two structural forms of the $n = 7$-9 cluster ions is presented. The anomalous behavior of C_7^+ is interpreted by an isomerization mechanism. Low-energy collision-induced dissociation studies of the primary product ions support a mechanism of carbene insertion into the H-CN bond and formation of covalently bonded products. In contrast, the HCN associates weakly with most primary product ions.

The emphasis of experimental and theoretical research on semiconductor and metal clusters in the last few years has been on the elucidation of their structures. A variety of experimental techniques has been applied in pursuit of this goal. With carbon cluster studies used as an example, these include: laser vaporization of thin foils or solid samples (which may be followed by a supersonic expansion) to generate and study the distribution of neutral and ionized clusters;[1-8] a fast-flow gas-phase reactor to study the reactivity of neutral clusters;[2] photodissociation of mass-selected positive cluster ions;[3] Fourier transform mass spectrometry (FTMS) to study the reactions of cluster ions;[4-6] metastable dissociation of positive cluster ions;[7] ultraviolet pho-

(1) Fürstenau, N.; Hillenkamp, F. *Int. J. Mass Spectrom. Ion Phys.* **1981**, *37*, 135-51. Rohlfing, E. A.; Cox, D. M.; Kaldor, A. *J. Chem. Phys.* **1984**, *81*, 3322-30. Bloomfield, L. A.; Geusic, M. E.; Feeman, R. R.; Brown, W. L. *Chem. Phys. Lett.* **1985**, *121*, 33-7.

(2) Zhang, Q. L.; O'Brien, S. C.; Heath, J. R.; Liu, Y.; Curl, R. F.; Kroto, H. W.; Smalley, R. E. *J. Phys. Chem.* **1986**, *90*, 525-8. Heath, J. R.; Zhang, Q.; O'Brien, S. C.; Curl, R. F.; Kroto, H. W.; Smalley, R. E. *J. Am. Chem. Soc.* **1987**, *109*, 359-63.

(3) Geusic, M. E.; Jarrold, M. F.; McIlrath, T. J.; Freeman, R. R.; Brown, W. L. *J. Chem. Phys.* **1987**, *86*, 3862-9. O'Brien, S. C.; Heath, J. R.; Curl, R. F.; Smalley, R. E. *J. Chem. Phys.* **1988**, *88*, 220-30.

(4) McElvany, S. W.; Creasy, W. R.; O'Keefe, A. *J. Chem. Phys.* **1986**, *85*, 632-3.

(5) McElvany, S. W.; Dunlap, B. I.; O'Keefe, A. *J. Chem. Phys.* **1987**, *86*, 715-25.

(6) McElvany, S. W. *J. Chem. Phys.* **1988**, *89*, 2063-75.

(7) Radi, P. P.; Bunn, T. L.; Kemper, P. R.; Molchan, M. E.; Bowers, M. T. *J. Chem. Phys.* **1988**, *88*, 2809-14.

(8) Yang, S. H.; Pettiette, C. L.; Conceicao, J.; Cheshnovsky, O.; Smalley, R. E. *Chem. Phys. Lett.* **1987**, *139*, 233-8. Yang, S.; Taylor, K. J.; Craycraft, M. J.; Conceicao, J.; Pettiette, C. L.; Cheshnovsky, O; Smalley, R. E. *Chem. Phys. Lett.* **1988**, *144*, 431-6.

toelectron spectroscopy (UPS) of negative cluster ions;[8] and electron spin resonance (ESR) spectroscopy of neutral clusters trapped in a matrix.[9] All of these methods have contributed to our current understanding of the structures and stabilities of carbon clusters.

FTMS is particularly well suited to the *quantitative* study of the chemistry of charged clusters.[4-6,10] This is due to its ability to isolate specific mass clusters (either positive or negative) and trap them for long times (seconds) to study their reactions. Chemical reactivity as a probe of ion structure has already been demonstrated to be a valid method.[11] Work in our laboratory[4] provided the first evidence for structural isomers of a semiconductor/metal cluster, C_7^+. More recently, Smalley and coworkers[8] have observed two distinct UPS spectra for the negative carbon clusters with 11, 50, 60, and 70 atoms, which they suggest also represent structural isomers. The other techniques mentioned above either do not produce isomeric forms of C_7^+ or are not sensitive to them.

Theoretical investigations into the structure of carbon clusters, C_n, have guided experiments and aided in the interpretation of results. Most of the theoretical work has focused on small neutral clusters, and only a few calculations have been carried out for the ionized clusters. Thus, the interpretation of experiments on cluster ions by neutral structural information must be done with care.

The earliest calculations found that the C_n were linear with a switch to monocyclic rings at $n = 10$.[12] This change in structure has been used to explain observed variations in reactivity,[4-6] photodissociation cross section,[3] and the UPS results.[8] Higher level MINDO/2 calculations[13] predicted that C_4 through C_7 had two or more stable isomers, with the most stable being the nonlinear isomer in each case. More recent ab initio configuration interaction calculations by Ray[14] have found the linear structure to be the most stable for neutral clusters with less than 10 carbon atoms. Other ab initio studies[15,16] predict that the cyclic isomers of C_4, C_6, and C_8 are the lowest in energy. The most complete ab initio calculation[17] on C_4 to date finds that the cyclic and linear isomers are essentially degenerate in energy; however, entropy will favor the linear form.

For the positive ions, Bernholc and Phillips[18] find that the clusters having less than 10 atoms are most stable in a linear configuration. Raghavachari and Binkley[16] disagree, predicting that C_4^+ and possibly C_6^+ and C_8^+ are cyclic. The odd n neutral and positive clusters are always predicted to be linear in the theoretical work mentioned above. Neutral C_3 is known experimentally to be linear,[19] but recent experiments suggest that C_3^+ is bent and may be cyclic.[20] Thus, a consensus on the structures of even the smallest clusters, not to mention the large clusters, has yet to be reached.

The proposed structures for the small ($n < 10$) cluster ions have reactive carbene sites (a pair of nonbonding electrons) at the end of the linear chains[18,21] as shown below

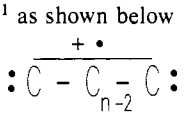

These are absent in the $n \geq 10$ cyclic structures. Evidence for this change in structure was obtained from previous experiments performed in our laboratory. The reactions of small carbon cluster ions, C_n^+ ($3 \leq n \leq 20$), with D_2 and O_2[5] and with CH_4, C_2H_2, and C_2H_4[6] were studied, and a large decrease in reaction rate constants between C_9^+ and C_{10}^+ was observed, consistent with this structural change. The C_7^+ ion reacts at two different rates, and it was postulated that two structural isomers were responsible for the observed differences in reactivity. By analogy to the change in reactivity at C_{10}^+ described above, the more reactive fraction of C_7^+ was assumed to be linear, while the slower reacting ions were assigned a cyclic structure.[4] In the previous work,[5] excess internal or translational energy was ruled out as the source of the biexponential decay observed for C_7^+.

In this article we extend our earlier work by examining the primary and secondary reactions of C_n^+ with HCN. HCN is an interesting contrast to the nonpolar reactants used previously as it is highly polar ($\mu_D = 2.98$ D) and also very polarizable ($\alpha = 2.59$ Å^3). Thus, the behavior of C_n^+ with HCN may be different from that observed for other C_n^+/neutral pairs. The reactions of HCN with small ($n < 5$) carbon cluster ions and their derivatives have been investigated by Anicich et al.[22] and Bohme et al.[23] These authors used electron impact on linear hydrocarbons to produce the reactant ions, while in the present work the ions are formed by direct laser vaporization of graphite. Results will be compared to examine the possibility that the two formation techniques may produce cluster ions that are structurally different.

The presence of HCN and HC_nN ($n < 12$) in interstellar molecular clouds[24] and other cosmic environments[25] is well documented, and a number of reaction schemes have been proposed for the synthesis of these large cyanopolyacetylenes.[26] Long-chain carbon molecules are also present in these clouds, and reactions with HCN could be part of a reaction scheme leading to formation of these molecules. In this paper, however, we will not attempt the integration of these reactions into the kinetic models for interstellar chemistry, as our emphasis will be on the chemistry of the carbon cluster ions.

Experimental Section

Experiments were performed in both a Varian I-T electromagnet and a Nicolet 3-T superconducting magnet Fourier transform ICR mass spectrometer (FTMS) using a Nicolet FTMS/1000 data system. The 3-T instrument is similar to the 1-T instrument described previously.[4,27] The 1-in. cubic cell is made of stainless steel plates except for the trapping plates, which are 90% transparent nickel mesh. The graphite sample is placed on a solids probe and inserted so it is flush with one of the trapping plates. The output of the frequency-doubled Quanta-Ray DCR-2 Nd:YAG laser (532 nm, 1-5 mJ/pulse, operated at 10 Hz) is focused by a 1-m lens, traverses the cell, and vaporizes the graphite sample to form carbon clusters (both neutrals and ions) by direct laser vaporization in

(9) Graham, W. R. M.; Dismuke, K. I.; Weltner, W. *Astrophys. J.* **1976**, *204*, 301-10. Van Zee, R. J.; Ferrante, R. F.; Zeringue, K. J.; Weltner, W., Jr.; Ewing, D. W. *J. Chem. Phys.* **1988**, *88*, 3465-74.
(10) Mandich, M. L.; Reents, W. D., Jr.; Bondybey, V. E. *J. Phys. Chem.* **1986**, *90*, 2315-9. Elkind, J. L.; Alford, J. M.; Weiss, F. D.; Laaksonen, R. T.; Smalley, R. E. *J. Chem. Phys.* **1987**, *87*, 2397-9.
(11) Leung, H.-W.; Ichikawa, H.; Li, Y.-H.; Harrison, A. G. *J. Am. Chem. Soc.* **1978**, *100*, 2479-84. Lifshitz, C.; Gibson, D.; Levsen, K. *Int. J. Mass Spectrom. Ion Phys.* **1980**, *35*, 365-70. Ausloos, P. J.; Lias, S. G. *J. Am. Chem. Soc.* **1981**, *103*, 6505-7. Smith, D.; Adams, N. G. *Int. J. Mass Spectrom. Ion Proc.* **1987**, *76*, 307-17.
(12) Hoffmann, R. *Tetrahedron* **1966**, *22*, 521-38.
(13) Slanina, Z.; Zahradnik, R. *J. Phys. Chem.* **1977**, *81*, 2252-7.
(14) Ray, A. K. *J. Phys. B.* **1987**, *20*, 5233-9.
(15) Whiteside, R. A.; Krishnan, R.; Defrees, D. J.; Pople, J. A. Schleyer, P. v. R. *Chem. Phys. Lett.* **1981**, *78*, 538-40. Magers, D. H.; Harrison, R. J.; Bartlett, R. J. *J. Chem. Phys.* **1986**, *84*, 3284-90. Rao, R. K.; Khanna, S. N.; Jena, P. *Solid State Commun.* **1986**, *58*, 53-6.
(16) Raghavachari, K.; Binkley, J. S. *J. Chem. Phys.* **1987**, *87*, 2191-7.
(17) Bernholdt, D. E.; Magers, D. H.; Bartlett, R. J. *Int. J. Quantum Chem.* **1988**, *S22*, in press.
(18) Berhnolc, J.; Phillips, J. C. *J. Chem. Phys.* **1986**, *85*, 3258-67.
(19) Gausset, L.; Herzberg, G.; Lagerqvist, A.; Rosen, B. *Discuss. Faraday Soc.* **1963**, *35*, 113-7.
(20) Faibis, A.; Kantner, E. P.; Tack, L. M.; Bakke, E.; Zabransky, B. J. *J. Phys. Chem.* **1987**, *91*, 6445-7.
(21) Raksit, A. B.; Bohme, D. K. *Int. J. Mass Spectrom. Ion Proc.* **1983**, *55*, 69-82.
(22) Anicich, V. G.; Huntress, W. T., Jr.; McEwan, M. J. *J. Phys. Chem.* **1986**, *90*, 2446-50.
(23) Bohme, D. K.; Dheandhanoo, S.; Włodek, S.; Raksit, A. B. *J. Phys. Chem.* **1987**, *91*, 2569-72.
(24) Morris, M.; Turner, B. E.; Palmer, P.; Zuckerman, B. *Astrophys. J.* **1976**, *205*, 82-93. Kroto, H. W.; Kirby, C.; Walton, D. R. M.; Avery, L. W.; Broten, N. W.; MacLeod, J. M.; Oka, T. *Astrophys. J.* **1978**, *219*, L133-7. Winnewisser, G.; Walmsley, C. M. *Astrophys. Space Sci.* **1979**, *65*, 83-93. Snell, R. L.; Schloerb, F. P.; Young, J. S.; Hjalmarson, Å.; Friberg, P. *Astrophys. J.* **1981**, *244*, 45-53.
(25) Hanel, R.; Conrath, B.; Flasar, F. M.; Kunde, V.; Maguire, W.; Pearl, J.; Pirraglia, J.; Samuelson, R.; Herath, L.; Allison, M.; Cruikshank, D.; Gautier, D.; Gierasch, P.; Horn, L.; Koppany, R.; Ponnamperuma, C. *Science* **1981**, *212*, 192-200. Irvine, W.; Hjalmarson, Å. *Cosmochemistry and the Origin of Life*; Ponnamperuma, C., Ed.; Reidel: Dordrecht, The Netherlands, 1983; pp 113-142.
(26) Bohme, D. K.; Włodek, S.; Raksit, A. B. *Can. J. Chem.* **1987**, *65*, 1563-7. Bohme, D. K.; Włodek, S.; Raksit, A. B. *Can. J. Chem.* **1987**, *65*, 2057-61.
(27) O'Keefe, A.; McDonald, J. R. *Chem. Phys.* **1986**, *103*, 425-36.

Table I. Branching Ratios and Rate Constants for the Primary Reactions of C_n^+ with HCN

reaction	cluster size (n) 3	4	5	6	7[a]	8[a]	9[a]	10	11 and 12	13	14–19	20
$C_n^+ + HCN \xrightarrow{k_p}$ $C_nH^+ + CN$	0.40 (0.04)[b]	0.26[c] (0.01)	0.30 (0.05)	0.06[c] (0.02)	0.13 (0.02)				NR[d]		NR	NR
$C_nCN^+ + H$	0.60 (0.04)	0.63 (0.02)	0.70 (0.05)	0.19 (0.06)	0.73 (0.02)		0.25 (0.04)					
$C_nHCN^+ + h\nu$		0.11 (0.02)		0.75 (0.06)	0.14 (0.01)	1.00	0.75 (0.04)	1.00		1.00		
k_p, 10^{-9} cm^3/s	1.27 (0.09)	1.12 (0.06)	1.14 (0.05)	0.86 (0.02)	1.15 (0.08)	0.68 (0.03)	0.77 (0.02)	2.36×10^{-4} (0.02)	$<6 \times 10^{-5}$	1.08×10^{-3} (0.20)	$<6 \times 10^{-5}$	$<8 \times 10^{-5}$

[a] Branching ratios and rate constants are for the most reactive fraction. See text for explanation. [b] 1σ error limits (in parentheses) are calculated from the set of measured values. [c] Branching ratios at small extent of reaction, as discussed in the text. [d] NR indicates this ion did not react. The upper limit of the rate constant is given.

a low-pressure environment. In the superconducting magnet the carbon clusters are ejected parallel to the magnetic field, instead of perpendicular as in the electromagnet.

In our previous cluster ion work,[4-6] the laser was triggered by the Nicolet computer at the beginning of an experimental cycle. For experiments in which the reaction time is varied, the operation of the laser (i.e. firing of the flash lamps etc.) is altered from the optimum repetition rate of 10 Hz. Frequent adjustments to the laser (e.g. flash-lamp power and tuning of the doubling crystal) were necessary to maintain constant laser output as the reaction time was changed. The longest reaction times that could be obtained in this configuration, using the 1-T electromagnet, were 1–2 s. These problems have been eliminated through the use of a microcomputer interfaced to the Nicolet computer, which now controls the timing of the laser, so that the flash lamps operate at the optimal 10 Hz and the Q-switch fires only when laser output is required.[28] These modifications, in conjunction with the higher field superconducting magnet, allow reaction times greater than 60 s to be used in the cluster ion experiments.

The resonant ejection capabilities of the FTMS allow us to completely isolate a particular mass ion for study. The rate constant is determined by following the pseudo-first-order decay of the reactant ion fraction as a function of time at constant HCN pressure. All reactions were studied to greater than 80% completion (and usually greater than 90%) except for a few cases where this was not possible due to the slowness of the reaction or low ion abundance. All first-order decay plots, except as noted later, were linear, though C_3^+ and several product ions required the addition of a buffer gas (Ar or Xe) and some delay time to remove excess translational and/or internal energy. The slope of this decay, divided by the HCN pressure, gives the rate constant.

The pressure is measured with a shielded ion gauge located approximately 0.5 m from the magnet. The background pressure in the vacuum chamber, which is pumped by a water-cooled Edwards Diffstak Series 160 diffusion pump, was $\leq 0.1 \times 10^{-8}$ Torr. The reactions were studied over a 10-fold pressure range, with typical corrected pressures being $(1-4) \times 10^{-7}$ Torr. The ion gauge pressure readings for HCN were corrected by measuring the rate constants for the reactions of three different ions with HCN at various pressures and comparing to the literature values.[29] The pressure correction factors obtained from each reaction did not depend on HCN pressure but did vary by a *factor of 2* among the three different reactions, even though ICR kinetic measurements from the same group were used as references. The average of the correction factors was used to determine the actual HCN pressure in our work. Due to this and other possible sources of error the absolute rate constants reported could be in error by as much as a factor of 2–3. However, the differences in the relative rate constants should be significant, as they were measured under similar conditions.

The HCN was made by reacting sodium cyanide with an excess of stearic acid under vacuum with gentle (80–90 °C) heating. The DCN was synthesized by slowly adding deuterated phosphoric acid (85% in D_2O, available from MSD Isotopes) to the solid sodium cyanide under vacuum. In each case, the product was trapped at liquid-nitrogen temperature as it was formed and then distilled from a liquid nitrogen/chloroform slush bath ($T = -63$ °C) to remove carbon dioxide. Electron ionization mass spectra of the purified samples showed no detectable impurities.

All results presented below are from the 3-T instrument. Its better ion-trapping ability and higher signal-to-noise ratio made it possible to study slower reactions and observe minor products. The preliminary results using the electromagnet are generally in good agreement with these results.

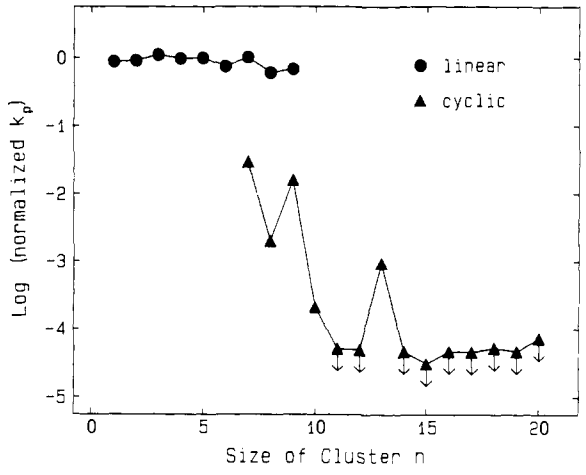

Figure 1. Rate constants k_p for the primary reactions of C_n^+ with HCN, normalized by the $n = 4$ rate constant, are plotted versus cluster size for the "linear" (●) and "cyclic" (▲) forms of the clusters. The values for C^+ and C_2^+, normalized by the C_4^+ reaction rate constant measured by Anicich et al.,[22] are included for completeness. Arrows on the triangles indicate these are upper limits.

Results

The rate constants and branching ratios were measured for the reactions of C_n^+ ($n = 3-20$) with HCN, as well as for the secondary reactions of all the primary reaction products. Collision-induced dissociation (CID) experiments to study the structure (bonding) of the product ions were also performed.

Primary Reactions. The products, branching ratios, and rate constants are given in Table I. The σ error limits are calculated from a set of 2–4 measured values. As noted in the Experimental Section, the reported absolute rate constants may be in error by a factor of 2–3 due to the uncertainty in the HCN pressure calibration. However, we expect the relative rates to be accurate within their error limits.

1. Rate Constants. The rate constants for the primary reactions, k_p, normalized by the rate constant for C_4^+ are plotted versus cluster size in Figure 1. As previously observed, there is a sharp drop in reactivity between C_9^+ and C_{10}^+, which has been attributed[4-6] to a change in structure from linear to cyclic. For $n = 10-20$, only C_{10}^+ and C_{13}^+ were observed to react, though their rates were near our limit of detectability. Also, as seen before, C_7^+ reacts at two different rates, with 70% of the C_7^+ reacting at a substantially slower rate. A new result, observed in this study, is that C_8^+ and C_9^+ exhibit similar behavior, with 30 and 20% of their cluster populations, respectively, reacting very slowly with

(28) Creasy, W. B.; Brenna, J. T. submitted in *Comput. Enhanced Spectrosc.*

(29) The reactions used for calibration were of CN^+, HCN^+, and CO_2^+ with HCN. Literature values were taken from: McEwan, M. J.; Anicich, V. G.; Huntress, W. T., Jr.; Kemper, P. R.; Bowers, M. T. *Int. J. Mass Spectrom. Ion Phys.* **1983**, *50*, 179–87. McEwan, M. J.; Anicich, V. G.; Huntress, W. T., Jr. *Int. J. Mass Spectrom. Ion Phys.* **1981**, *37*, 273–81.

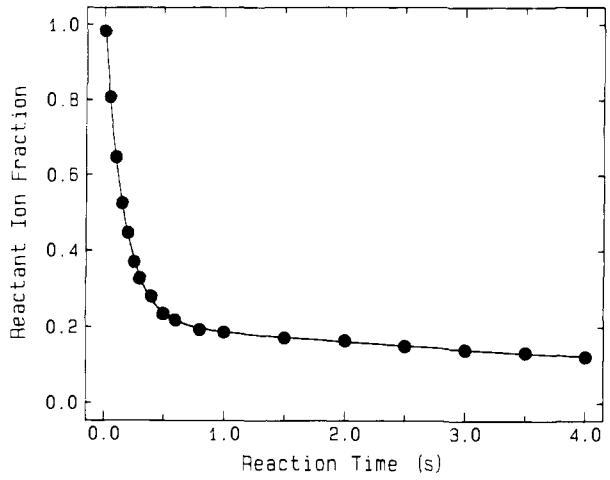

Figure 2. Decay of C_9^+ reacting with HCN is shown as a function of reaction time. The line is a biexponential fit to the data. The errors bars for the points are equal to or smaller than the point size.

Table II. Parameters of the Biexponential Decay Model, for the Reactions of C_7^+, C_8^+, and C_9^+ with HCN

size of cluster	F_{slow}	k_{fast}/k_{slow}
7[a]	0.68 ± 0.03[b]	36 ± 5
8	0.30 ± 0.02	300 ± 54
9	0.20 ± 0.01	43 ± 3

[a] As explained in the text, the decay curve for C_7^+ is not a true biexponential. Parameters given are for the best biexponential fit. [b] 1σ error limits are calculated from the set of measured values.

HCN. (The slow decrease of k_p with n for the HCN reactions, and the instrumental changes described in the Experimental Section, made it possible to detect the less reactive fractions of C_8^+ and C_9^+ in this work. Recent studies of C_8^+ and C_9^+ with D_2 have reproduced the isomer populations observed in this study.) An example of the C_9^+ decay plot is shown in Figure 2. The solid line is a nonlinear, least-squares fit of the data using a biexponential decay model

$$[C_n^+]_t/[C_n^+]_0 = F_{fast}\exp(-k_{fast}t) + F_{slow}\exp(-k_{slow}t) \quad (1)$$

The left side of eq 1 is the fraction of reactant ions remaining at time t. F_{fast} and F_{slow} are the fractions of the two components of the decay, with the corresponding rate constants k_{fast} and k_{slow}. A summary of the parameters for the biexponential fits for C_7^+, C_8^+, and C_9^+ is given in Table II. As discussed in the introduction, C_7^+ is believed to exist as both linear and cyclic isomers in the direct laser vaporization experiment. MNDO calculations[5] of the difference in the heat of formation of the cyclic and linear structures of C_n^+, ΔH_f(cyclic C_n^+) − ΔH_f(linear C_n^+) > 0, indicate that this quantity decreases with n for $n > 5$. Thus, it is not surprising to also observe two isomeric forms for C_8^+ and C_9^+. In the rest of the article, we will refer to the more reactive n = 3–9 cluster ions as "linear" and the less reactive n = 7–20 cluster ions as "cyclic".

Considering only the linear clusters for the moment, Table I indicates that all reactions are fast, with only a factor of 2 variation in the reactivity for the n = 3–9 clusters. This is in contrast with O_2 and D_2, for which the rate constants vary by a factor of 30–70, respectively.[5] The reactions with CH_4, C_2H_2, and C_2H_4 show variations of factors of 4–6 in the rate constants.[6] The odd/even staggering of rate constants noted in previous work is also observed for the HCN reactions, though it is weaker.

The cyclic clusters show quite pronounced changes in reactivity of over 2 orders of magnitude. Again, it is the odd clusters that are more reactive. The relatively high reactivity observed for C_{13}^+ has been correlated with its low abundance in the nascent cluster ion distribution.[6] The low reactivity of C_{10}^+ with HCN (k_p = 2.4×10^{-13} cm^3/s) contrasts sharply with the rate constants of $\sim 5 \times 10^{-10}$ cm^3/s measured for the reactions with C_2H_2 and C_2H_4.[6] In general, HCN reactivity resembles that of the hydrocarbons. All of these species are highly reactive and show little variation in reactivity with cluster size for the linear isomer.

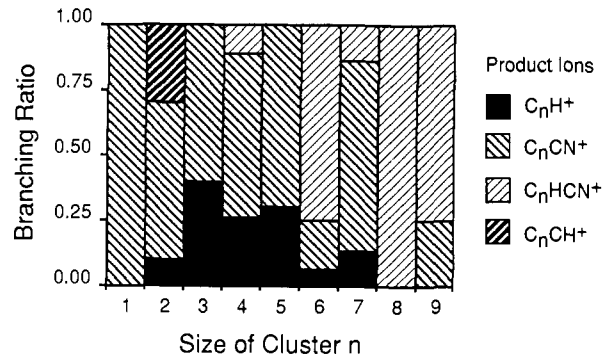

Figure 3. Branching ratios for the primary reactions of the linear carbon cluster ions with HCN are plotted. The results for the C^+ and C_2^+ reactions were taken from ref 22.

2. Reaction Products and Branching Ratios. Only three different reaction channels are observed in the HCN reactions, as shown in Table I. These reactions can be visualized as an association of the C_n^+ with HCN to form the reaction intermediate, followed either by stabilization of the adduct to form the association product (see the Discussion) or by expulsion of an H or CN neutral. Fragmentation of the reactant carbon cluster ion was not observed. This contrasts with most previous studies[4-6] in which significant amounts of cluster fragmentation products were formed. Reactions with CO studied by the selected ion flow tube (SIFT) technique produce only the association products,[30] presumably due to stabilization of the reaction complex by collisions with the high-pressure buffer gas.

For ease of comparison, the branching ratios of the product ions from the reactions of the linear clusters are plotted in Figure 3. For C_4^+ and C_6^+ the measured branching ratio varies with reaction time, due to multiple pathways leading to the same product (e.g. C_nHCN^+ is both a primary product and a secondary product from C_nH^+ and C_nCN^+). For C_7^+ and C_9^+ the apparent time variation in the branching ratio is due to the two isomeric forms reacting at different rates to give different products. The values in Table I and Figure 3 represent initial branching ratios determined at small (<10%) extent of reaction when these complicating reactions are least significant and extrapolated to zero reaction time. The cyclic isomers form only the association product.

The branching ratios for the linear clusters show several superimposed trends. The first is that the smaller clusters stabilize after association by eliminating a fragment of the HCN (i.e. H or CN). The larger clusters can accommodate the excess energy long enough for the adduct to stabilize, possibly by emitting IR photons. The second is that C_nCN^+ is the favored product of all dissociating adducts. The third is that the even cluster ions add HCN more readily than the odd clusters (for example, compare the branching ratio for HCN addition of C_7^+ to those of C_6^+ and C_8^+).

It is interesting to note the facility with which the larger linear clusters (n = 6, 8, and 9) form the association product. This was not observed in any of the previous studies of carbon cluster ion reactions. The strong ion–dipole and ion–induced dipole interactions in the [C_n^+·HCN] complex increase both the lifetime of the complex and the probability of stabilizing the adduct, either by collisions or by radiative emission.

Secondary Reactions. While the primary reactions were studied, secondary product ions were also observed. The secondary reactions were investigated in the same way as the primary reactions; i.e. the reactant ion, which is the product ion of a primary reaction, was isolated, and the reaction rate constants, products, and branching ratios were determined in an unambiguous manner. We studied the reactions of all the observable primary product

(30) Bohme, D. K.; Włodek, S.; Williams, L.; Forte, L.; Fox, A. *J. Chem. Phys.* **1987**, *87*, 6934–8.

Table III. Branching Ratios and Rate Constants for the Secondary Reactions of C_n^+ with HCN

reactio	cluster size (n) 3	4	5	6	7	8	9
$C_nH^+ + HCN \xrightarrow{k_s}$							
$\rightarrow C_nH_2^+ + CN$		0.14		0.04		NF[a]	NF
$\rightarrow C_nHCN^+ + H$		0.86		0.53			
$\rightarrow C_nH_2CN^+ + h\nu$	0.91		1.00	0.43	1.00		
$\rightarrow H_2CN^+ + C_n$	0.09						
k_s, 10^{-9} cm^3/s	0.040	1.01	0.091	0.507	0.424		
$C_nCN^+ + HCN \xrightarrow{k_s}$							
$\rightarrow C_nHCN^+ + CN$		0.27		0.05		NF	
$\rightarrow C_n(CN)_2^+ + H$		0.57		0.21			
$\rightarrow C_nH(CN)_2^+ + h\nu$	1.00	0.16	1.00	0.74	1.00		1.00
k_s, 10^{-9} cm^3/s	0.378	0.942	0.377	0.173	0.170		0.177
$C_nHCN^+ + HCN \xrightarrow{k_s}$							
$\rightarrow C_n(HCN)_2^+ + h\nu$	NF	NR[b]	NF	NR	1.00[c]	NR[c]	NR[c]
k_s, 10^{-9} cm^3/s		$<3.2 \times 10^{-4}$		$<5.0 \times 10^{-4}$	3.1×10^{-3}	$<5.6 \times 10^{-4}$	$<7.0 \times 10^{-4}$

[a] NF indicates this reactant ion is not formed by the primary reaction. [b] NR indicates this ion did not react. The upper limit for the rate constant is given. [c] The C_nHCN^+ are produced from a mixture of the "cyclic" and "linear" C_n^+.

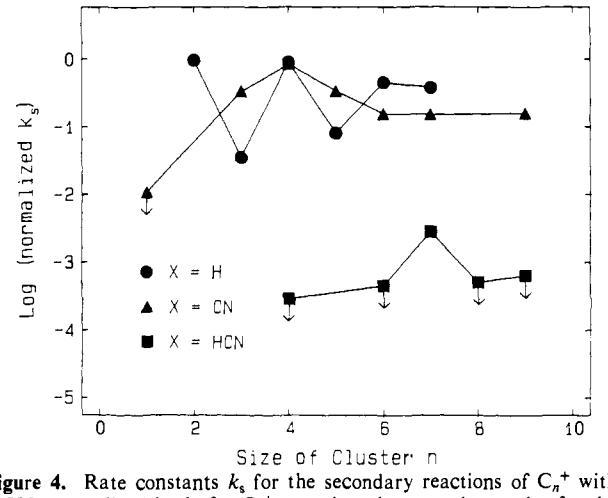

Figure 4. Rate constants k_s for the secondary reactions of C_n^+ with HCN, normalized by k_p for C_4^+, are plotted versus cluster size for the three series of reactant ions C_nX^+ (X = H, CN, or HCN). The values for the C_2H^+ and CCN^+ reactions were taken from ref 22 and 29, respectively. Symbols with arrows are upper limits.

ions, which are of three types, C_nH^+, C_nCN^+, and C_nHCN^+. Reactions were studied to 80–95% completion in most cases, and no evidence for isomeric forms of the primary product ions was found in these secondary reactions. The results are summarized in Table III.

1. Rate Constants. The reaction rate constants for each series of reactant ions, k_s, normalized by k_p for C_4^+ are shown in Figure 4.

C_nH^+ shows very large even/odd alternations in rate constant, with the even clusters being more reactive than the odd clusters. For comparison, consider the reactions of C_nD^+ with D_2 and of C_nH^+ with C_2H_2, which have been studied previously. The C_nD^+ reactions show large even/odd alternations in rate constants (essentially reaction/no reaction) although the absolute reactivity is relatively low.[5] (The largest rate constant is 8×10^{-11} cm^3/s for the reaction of C_4D^+ with D_2.) The C_nH^+ are fairly reactive with C_2H_2, but the even/odd variation is small.[6] The C_nH^+/HCN reaction has characteristics of both these examples, showing high reactivity like the C_2H_2 reactions, combined with a pronounced size dependence as in the D_2 reactions.

The C_nCN^+ ions are all moderately reactive. The even/odd alternation in rate constants persists only for n = 3–5, with a maximum value for C_4CN^+, before leveling off.

C_nHCN^+ ions were unreactive at our detection limits, with the exception of C_7HCN^+ formed from the cyclic C_7^+, which has a measured rate constant of 3×10^{-12} cm^3/s. For the linear ions, one possible explanation for this nonreactivity is that, after insertion of the carbene into the H–CN bond, the H migrates to the other end of the chain to give the structure HC_nCN^+, thus blocking the second carbene site. The CID results discussed below give further information on the structure.

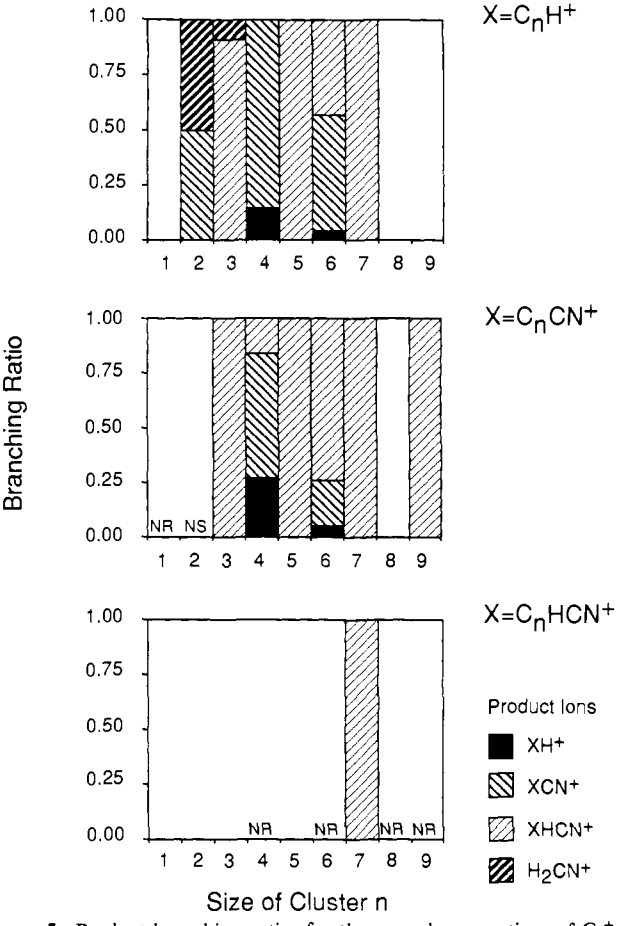

Figure 5. Product branching ratios for the secondary reactions of C_n^+ with HCN are shown. In the top figure the reactant ion X is C_nH^+, in the middle figure it is C_nCN^+, and in the bottom figure X is C_nHCN^+. Results for the reactions of n = 1 and 2 ions are from the literature.[22,29] Ions that were nonreactive are indicated by NR. C_2N^+ was found to be nonreactive under low-pressure conditions[29] but to undergo three-body association at high pressures.[37] The reaction of C_2CN^+ has not been studied and is marked NS. Blank spaces indicate that the reactant ion was not formed in the primary reaction.

2. Reaction Products and Branching Ratios. The branching ratios of the secondary reaction products are shown in Figure 5. Each bar graph is for one series of reactant ions and gives the product distribution for each reaction. Products resulting from

the breakup of the carbon cluster were not observed in any of the reactions. Also, no tertiary products were observed.

It is immediately apparent that many of the ions react by association with HCN, whether the ion is C_nH^+, C_nCN^+, or C_nHCN^+. What is striking is that, with one exception, only even n ions form other products, either addition of H or CN. This may indicate that these reactions are more exothermic than those of the odd n ions. The exception is C_3H^+, which gives a small amount of proton transfer to HCN. CH^+ and C_2H^+ also proton transfer to HCN,[22] while C_4H^+ and the larger members of the series do not. This places the proton affinity of HCN (7.43 eV) between those of C_3 and C_4.

Collision-Induced Dissociation. CID studies were carried out for about half of the product ions to obtain information on the bonding of the primary and secondary reaction products and relative bond strengths. (The signal-to-noise ratio was too low for the remaining ions to be successfully studied.) The ion to be dissociated was excited by a short, low-intensity radio-frequency pulse to give calculated maximum translational energies in the range of 3–100 eV (lab). Collisions with the Xe buffer gas led to dissociation of the ion. The measured Xe pressure was (5–10) $\times 10^{-7}$ Torr. The corrected pressure is several times higher.

1. CID of Primary Product Ions. The primary reaction products C_nH^+ and C_nCN^+ dissociate essentially by the loss of H and CN, respectively. (Some loss of the stable neutral C_3 is also observed at higher energies for C_3CN^+ and C_7CN^+.) Thus, the weakest bond in the primary product ion is the new bond formed with the H or CN fragment. This is in agreement with the observed lack of cluster breakup in the primary reactions.

The linear C_nHCN^+ (n = 4, 6–9) fragment to lose H and CN, as well as some HCN (most likely as H + CN) at higher excitation energies. Loss of C_3 and C_3H is also observed at slightly higher excitation energies for n = 8 and 9. The observed loss of C_3 makes the HC_nCN^+ structure for these ions unlikely since it would require extensive rearrangement during the CID process. It is important to note that the ions produced in the low-energy CID processes are the same as those formed by ion–molecule reactions, suggesting that C_nHCN^+ is the stabilized intermediate of these reactions.

The CID mass spectra of the cyclic C_nHCN^+ (n = 8–10 and 13) are quite different from those of the linear C_nHCN^+. For the cyclic adduct ions the facile loss of *only* HCN is observed with just a few electron volts of excitation energy, which is 5–10 times smaller than the energies required for dissociation of the linear adduct ions. Obviously, the linear and cyclic association product ions do not have the same structure. The linear adduct ions fragment in a way consistent with insertion into the H–CN bond and formation of covalent bonds to H and CN, while the cyclic ions associate only weakly with HCN. The dissociation of cyclic C_7HCN^+, however, closely resembles that of the linear adduct ions, losing H and CN at much higher excitation energy.

2. CID of Secondary Product Ions. Most of the secondary product ions could not be studied by CID due to insufficient signal. Of those ions studied, all but one were of the type C_nXHCN^+ (where X is H, CN, or HCN). Without exception, the CID of these ions gave exclusively HCN loss observable at fairly low excitation energies. These energies are approximately the same as those required for the fragmentation of the cyclic C_nHCN^+ and much lower than those required for the corresponding C_nX^+ CID.

For the product ion $C_7(HCN)_2^+$, derived from cyclic C_7^+, one might ask if the two HCN are equivalent. The CID results seem to indicate otherwise. The HCN added in the primary reaction is lost as H or CN at higher energies than the HCN added in the secondary reaction, which is weakly bound and lost as HCN. The nature of the HCN bonding to the cluster ion in $C_7(HCN)_2^+$ was further probed by using a mixture of HCN and DCN to perform the following experimental sequence:

$$\text{cyclic } C_7^+ \xrightarrow[DCN]{k_p} C_7DCN^+ \xrightarrow[HCN]{k_s} C_7(DCN)(HCN)^+ \xrightarrow[Xe]{CID} C_7DCN^+ + HCN$$

Only fragmentation to lose HCN was observed at low CID excitation energies. This indicates that the two HCN's are bound to nonequivalent sites, that they do not exchange, and that the second HCN to bond is the more weakly bound and the first to be lost by CID. Coupled with the observation that most secondary reactions only add HCN, the CID results indicate that a second HCN does not usually react with the remaining carbene end of the C_nX^+ to form covalent bonds. The interaction is much weaker, possibly with the X end of the ion and explains the predominance of HCN association in the secondary reactions. This will be considered in more detail in the Discussion.

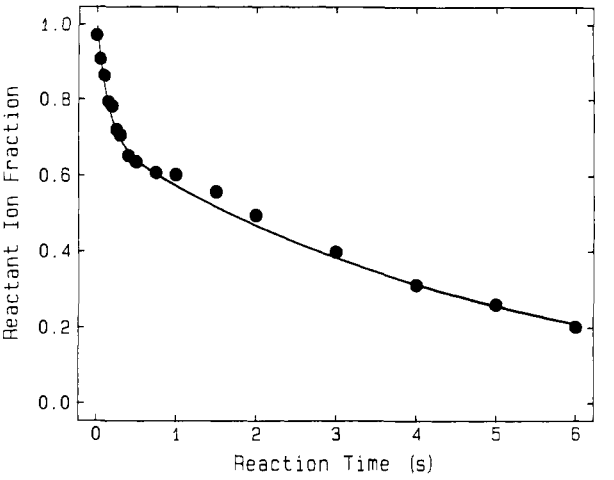

Figure 6. Decay of C_7^+ reacting with HCN is plotted as a function of reaction time. The line is a biexponential fit to the data, including points for reaction times up to 10 s, which are not shown here. The error bars are equal to or smaller than the point size. Note the "hump" between 1- and 2-s reaction times.

It would be interesting to study an ion of the type C_nHCN^+ formed by different pathways (e.g. addition of HCN via association versus addition of H and CN in two sequential steps) to see if any differences in bonding could be observed. Both C_4^+ and C_6^+ make this ion via three pathways; however, in each case only C_nHCN^+ from the primary (i.e. association) reaction could be studied. The branching ratios were not favorable, and the yield of these ions from the secondary reactions were too low to perform the CID experiments.

Discussion

The C_7^+ Anomaly. In this study we have observed three distinct types of kinetic behavior. One set of ions, C_3^+–C_9^+, react rapidly with HCN to form covalent bonds at the carbene site. In most cases, a second HCN can also react at the remaining carbene site or associate with the ion. The most likely structure for these ions is linear. Another group of ions, C_8^+–C_{10}^+ and C_{13}^+, react slowly with HCN to form a weakly bound adduct. Calculations suggest that these ions have a monocyclic structure. The cyclic C_7^+ differs from all other carbon cluster ions and exhibits the following unusual behavior: (1) the cyclic fraction is much higher for C_7^+ than for C_8^+ and C_9^+, (2) its adduct, C_7HCN^+, is more reactive than the other C_nHCN^+, (3) the CID fragmentations and the energies required for fragmentation are the same for cyclic and linear C_7HCN^+, indicating strong covalent bonding in the cyclic adduct, instead of the weak associative bonding seen for the other cyclic C_nHCN^+ (n = 8–10 and 13), and (4) the shape of the C_7^+ decay curve is not a simple biexponential as was found for C_8^+ and C_9^+ (see Figure 2).

Considering the last point, a typical decay curve for C_7^+ is shown in Figure 6. The solid line is the biexponential fit to the data given by eq 1. Between 1 and 2 s reaction time the data points lie above the fitted line, giving the curve a "humped" appearance. This hump is a consistent feature in all the C_7^+ decay curves measured, at an approximately constant value of the pressure × time product. Zakin et al.[31] have observed a similar phenomena

(31) Zakin, M. R.; Brickman, R. O.; Cox, D. M.; Kaldor, A. *J. Chem. Phys.* **1988**, *88*, 3555–60.

in their study of niobium clusters. In particular, the decrease in Nb_{12}^+ as a function of reactant concentration showed two reaction regions separated by a plateau. They postulate that this plateau is due to an "induction" period during which time there are not enough collisions to result in an observable decay in the reactant species. The shape of the curve in Figure 6 suggests it is the sum of a fast, single-exponential decay and a more complex function. This function initially rises and then exponentially decays with a rate slower than that of the fast, single-exponential decay.

One possible mechanism to explain this behavior is the following:

$$C_{7A}^+ + HCN \rightarrow \text{products} \quad (2a)$$

$$C_{7B}^+ + HCN \rightarrow C_{7C}^+ + HCN \quad (2b)$$

$$C_{7C}^+ + HCN \rightarrow C_{7C}HCN^+ \quad (2c)$$

C_{7A}^+ is the linear form, which reacts rapidly. Note that reaction 2a is not coupled to the rest of the kinetic scheme. Reactions 2b and 2c represent the behavior of C_{7B}^+, which undergoes "activation" by collisions with HCN. The adduct of HCN with the B form is not stable whereas that with the C form is. The C and A ions are also not identical, at least energetically, as they do not form the same products. (See the previous section on the results of the primary reaction branching ratios.)

The slow-reacting C_7^+ (and also C_8^+ and C_9^+) is not an excited state of the fast-reacting linear isomer, which relaxes by collisions. Previous experiments[5] to probe for the existence of metastable C_7^+ by variation of reactant pressure indicated that such a state would need to be extremely long-lived (τ_{rad} greater than several seconds), which seems unrealistically long for a species of this size. The observed isomer fractions of C_7^+–C_9^+ are also invariant with HCN pressure and in the presence of excess Xe (100:1 Xe/HCN) to quench any electronically excited species prior to reaction with HCN. Also, the fraction of C_7^+–C_9^+ in the excited state would probably be sensitive to the formation conditions, (e.g. laser output), which has not been observed.

Reactions 2b and 2c suggest that C_{7B}^+ isomerizes during the reaction with HCN, i.e. from the cyclic to the linear form. This is consistent with points 2–4 listed above but does not account for the large fraction of cyclic isomer (point 1). Another possibility is that the more abundant C_7^+ fraction has a different structure than those already noted. The MNDO calculations performed for a previous study[5] considered several C_7^+ structures, including branched chains and rings. Except for the monocyclic ring, no isomers have energies within several electron volts (at this level of calculation) of the most stable linear form. Our conclusion is that a cyclic to linear isomerization best explains our results.

Prediction of Trends in Reactivity and Branching Ratios. Using Hückel theory, with hybridization and electron correlation included, Leleyter and Joyes[32] have calculated relative energies of neutral and ionized linear M_pC_n clusters, where M is a variety of metallic or nonmetallic elements. With these results and the "correspondence rule", they have accounted for the patterns in the experimental abundances of many types of substituted carbon clusters. The correspondence rule[32] states that *observed strong (weak) intensities of cluster ions correspond to high (low) stabilities of these clusters*. The most stable clusters are those with a full, or nearly full, HOMO (highest occupied molecular orbital). For carbon clusters and many substituted carbon clusters, the HOMO falls in a doubly degenerate π molecular orbital band.[32] We have used the results of Leleyter and Joyes, and extended them to related clusters, to explain the observed variations in the reactivity trends and in the branching ratios of the HCN reactions.

From the trends in reactivity with cluster size for all the reactions of C_n^+ and C_nX^+ studied to date, we formulate the following empirical rule: *For an odd electron series, the odd n ions will be more reactive than the even n ions, and vice versa, irrespective of the neutral reactant.* (Note that for any series of ions C_n^+ or C_nX^+, the parity of the number of electrons is the same for all the ions in a series.) By this rule, for C_n^+ and C_nO^+ odd n ions will be more reactive whereas the even n ions will be more reactive for C_nH^+ (C_nD^+) and C_nCN^+. This is generally what has been observed in this and previous studies[4-6] and can be explained by the Hückel model.

Even electron ions (C_nH^+, C_nCN^+) have filled HOMOs for odd n and half-filled HOMOs for even n. The open-shell ions should be the more reactive, as is observed. The odd electron ions (C_n^+, C_nO^+) are open-shell species for n both even and odd. The odd n ions, with three electrons in the HOMO, can complete their HOMO and so are more reactive than the even n ions in the series.

The observed branching ratios of the HCN reactions can also be explained with the Hückel model and the correspondence rule. Restating the correspondence rule for reactions, the more stable product ions are expected to show larger branching ratios when comparing a homologous series of reactions. In the primary reactions of C_n^+ with HCN, the theory predicts that addition of H and CN will be favored for odd n reactants. The experimental results in Table I are in good agreement with this prediction. HCN can add to C_n^+ to form either $C_n(H)CN^+$, for which odd n are more stable, or HC_nCN^+, which are more stable when n is even. Experimentally, larger branching ratios for association are observed for the even n reactants. This can be interpreted in two ways. The adducts, especially the even n ions, have the HC_nCN^+ structure. This also explains the lack of observed secondary reactions for most of these ions. The n = 7 and 9 products, however, may retain the $C_n(H)CN^+$ structure. Another explanation considers that one intermediate in the primary reactions is $[C_n(H)CN^+]$. The odd n species are more likely to form other products (i.e. C_nH^+ and C_nCN^+). Thus, the even n clusters only appear to produce more of the association product.

The theory is applicable only to linear, covalently bound molecules. Thus, the only secondary reactions we can consider are those of C_nH^+ and C_nCN^+ to add H or CN. The four ion products formed are more stable for even n reactants. Indeed, Table III shows that these reactions occur only for n = 4 and 6.

For the simple reactions discussed above, the modified Hückel theory can predict which ions in a homologous series will be the most reactive and which products are most likely to be formed. This suggests that energetics is the determining factor in the thermal reactions of carbon and substituted carbon cluster ions.

Structures of Product Ions. As already noted, the reactions of C_n^+ with HCN were the first to be studied in which no breakup of the carbon cluster is observed. The reactant H–CN bond is relatively strong (120 kcal/mol), and the CID results show that the bonds formed to CN and H are the weakest bonds in the product ion. The observation of significant amounts of association products supports the conclusion that the energy in the $(C_n{\cdot}HCN)^+$ complex must be low.

Reaction by the addition of a second HCN is observed, but no tertiary products are formed. This appears to agree with the postulated mechanism of reaction at the two carbene sites of the linear chain. However, the CID results partially contradict this interpretation. The first HCN addition does appear to occur at the carbene site, bonding covalently. In the secondary reactions, addition of HCN is the dominant channel for reaction. The CID studies showed that this HCN is probably not covalently bound at the remaining carbene end of the ion. Instead, the bonding may be similar to that found in van der Waals complexes of HCN, both with itself and unsaturated hydrocarbons. The neutral HCN dimer has the linear structure HCN···HCN with a relatively strong binding energy[33] of 1540 cm^{-1}. Analogously, the HCN may bind to the CN of C_nCN^+ or C_nHCN^+. For the adducts of C_nH^+ with HCN, the situation is less clear. Spectroscopic studies of the complexes of HCN with acetylene, ethylene, and cyclopropane show that they are T-shaped, as the HCN orients itself H end first, perpendicular to the bond between two carbons.[34] The

(32) Leleyter, M.; Joyes, P. *J. Phys. (Les Ulis, Fr.)* **1975**, *36*, 343–55. Joyes, P.; Leleyter, M. *J. Phys. (Les Ulis, Fr.)* **1984**, *45*, 1681–8. Leleyter, M.; Joyes, P. *Surf. Sci.* **1985**, *156*, 800–13. Leleyter, M. *J. Phys. Lett.* **1985**, *46*, L915–22. Leleyter, M., to be submitted for publication in *Z. Physik D.*

(33) Buxton, L. W.; Campbell, E. J.; Flygare, W. G. *Chem. Phys.* **1981**, *56*, 399–406.

Table IV. Comparison of Results for the Reactions of C_3 and C_4 Ions with HCN

reaction	FTMS[a]	ICR[b]	SIFT[c]
$C_3^+ + HCN \rightarrow C_3H^+ + CN$	0.40 ± 0.04		
$\rightarrow C_3CN^+ + H$	0.60 ± 0.04	1.0	
rate constant[d]	1.27 ± 0.09		
$C_3H^+ + HCN \rightarrow C_3H_2CN^+ + h\nu$	0.91 ± 0.04	0.5	1.0
$\rightarrow H_2CN^+ + C_3$	0.09 ± 0.04	0.5	
rate constant	0.040 ± 0.004	0.13 ± 0.01	1.1 ± 0.3
$C_3CN^+ + HCN \rightarrow C_3H(CN)_2^+ + h\nu$	1.00		1.0
rate constant	0.378 ± 0.006		0.84 ± 0.25
$C_4^+ + HCN \rightarrow C_4H^+ + CN$	0.26 ± 0.01	0.3	
$\rightarrow C_4CN^+ + H$	0.63 ± 0.02	0.5	
$\rightarrow C_4HCN^+ + h\nu$	0.11 ± 0.02	0.2	
rate constant	1.12 ± 0.06	2.8 ± 0.3	
$C_4H^+ + HCN \rightarrow C_4H_2^+ + CN$	0.14 ± 0.02		
$\rightarrow C_4HCN^+ + H$	0.86 ± 0.02	0.95	
$\rightarrow C_4H_2CN^+ + h\nu$		0.05	
rate constant	1.01 ± 0.06	1.7 ± 0.2	

[a] This work. [b] Reference 22. [c] Reference 23. [d] All rate constants are in units of 10^{-9} cm^3/s. FTMS 1σ error limits are statistical and calculated from the set of measured values.

binding energy of HCN with these hydrocarbons is much weaker, ranging from 575 to 862 cm^{-1}. With CO the HCN does not search out the π bond, preferring instead the linear or slightly nonlinear configuration[35] OC···HCN. The binding energy of this complex is similar to those measured for the hydrocarbon complexes. Since the effect of the charge on the complexing has not been taken into account, one cannot rule out other structures that may be more stable for the ions.

Literature Comparisons. As was mentioned in the introduction, calculations have predicted low-energy cyclic structures for the smaller clusters, especially C_4^+. Comparison of our results for the C_3^+ and C_4^+ reactions with literature values may indicate whether the different formation techniques employed (direct laser vaporization of graphite versus electron impact on linear hydrocarbons) lead to different cluster structures and reactivities. The data for this comparison are given in Table IV. Our measured rate constants are consistently lower than those of Anicich et al.[22] and Bohme et al.[23] by a factor of 2–3. This cannot be accounted for by the uncertainty in the pressure calibration factor.

Comparison of the branching ratios shows significant differences for the reactions of C_3^+ and C_3H^+. Minor differences are seen in the branching ratios of the C_4^+ and C_4H^+ reactions. The previous ICR experiments[22] did not observe the addition of H to C_3^+ (possibly due to the low reactant ion intensity) and to C_4H^+ (a minor pathway). The C_3H^+ reaction in our experiment produced 90% association product, which agrees with the SIFT[23] but not the ICR[22] results. If we use the amount of association product formed as an indicator of excess internal energy in the reactant ion, C_4^+ and C_4H^+ appear to have some excess internal energy in these FTMS experiments, while C_3H^+ seems to have been internally excited in the ICR experiment.

The question arises as to whether the observed differences in rate constants and branching ratios are due to structural differences of the ions produced in the different experiments. Since internal excitation of the ions in the various experiments can account for the results, it is difficult to attribute the observed differences to linear/cyclic structures in the absence of more conclusive evidence. Note that, in the work by Faibis et al., the C_3^+ was formed by electron impact on linear hydrocarbons, but the results indicate the ion has a bent geometry.[20]

Radiative Association. The formation of larger species by radiative association has been postulated to play an important role in the chemistry of the interstellar medium.[36] In the Results, it was noted that many of the reactions studied produced the association product for reactant ions ranging in size from C_3H^+ up to C_{13}^+. Most of the association rate constants measured are greater than 1×10^{-10} cm^3/s. Even a large three-body rate constant of 1×10^{-22} cm^6/s, at a pressure of 3×10^{-7} Torr, would correspond to an apparent bimolecular rate constant of only 1×10^{-12} cm^3/s. Only the very slowest reactions (those of cyclic C_8^+, C_{10}^+, C_{13}^+, and C_7HCN^+) have rate constants in this range. Thus, the contribution of three-body reactions to the measured rates is not expected to be significant.

The experiments were performed at pressures in the low 10^{-7} Torr range, giving an average time between collisions that varies from 80 ms down to 35 ms. If the unstabilized adduct survives this long, it may be stabilized by subsequent collisions with the HCN. To investigate this possibility, the reaction of linear C_8^+ with HCN was studied at HCN pressures ranging from 2.6×10^{-8} to 8×10^{-7} Torr. (Each HCN pressure reading was calibrated by the reaction of HCN^+ with HCN, to eliminate any effects arising from the pressure correction.) The average time between collisions varies from 490 to 16 ms over this pressure range. All of the measured rate constants were within 20% of the average value and did not vary systematically with HCN pressure. The stability of the C_8HCN^+ adduct ion in the absence of collisions was studied at low HCN pressure by resonant frequency ejection of the reactant C_8^+ (requiring 3–5 ms) following short reaction times (~5–10% extent of reaction). The C_8HCN^+, which is isolated, is not observed to back-dissociate to C_8^+ and HCN and thus is not metastable on this time scale. These results indicate that subsequent stabilizing collisions with HCN are not necessary for the C_8HCN^+ adduct to be formed and detected. It also puts an upper limit of approximately 10–20 ms on the lifetime of the initially formed collision-complex, prior to stabilization. Thus, we are confident that the mechanism responsible for the formation of the adducts must be radiative association.

The size of the adducts (≥7 atoms) as well as the strong ion–dipole and ion–induced dipole interactions are factors that are conducive to the formation of long-lived complexes. Since temperatures in the interstellar medium are much lower, which increases the probability of radiative association taking place, re-

(34) Aldrich, P. D.; Kukolich, S. G.; Campbell, E. J. *J. Chem. Phys.* **1983**, *78*, 3521–30. Kukolich, S. G.; Read, W. G.; Aldrich, P. D. *J. Chem. Phys.* **1983**, *78*, 3552–6. Kukolich, S. G. *J. Chem. Phys.* **1983**, *78*, 4832–5.
(35) Goodwin, E. J.; Legon, A. C. *Chem. Phys.* **1984**, *87*, 81–92.

(36) Herbst, E.; Schubert, J. G.; Certain, P. R. *Astrophys. J.* **1977**, *213*, 696–704. Freeman, C. G.; Harland, P. W.; McEwan, M. J. *Astrophys. Lett.* **1978**, *19*, 133–5. Smith, D.; Adams, N. G. *Astrophys. J.* **1978**, *220*, L87–92. Huntress, W. T., Jr.; Mitchell, G. F. *Astrophys. J.* **1979**, *231*, 456–67. Schiff, H. I.; Bohme, D.K. *Astrophys. J.* **1979**, *232*, 740–6.
(37) Freeman, C. G.; Harland, P. W.; Liddy, J. P.; McEwan, M. J. *Aust. J. Chem.* **1978**, *31*, 963–6.

actions of HCN with ions such as C_n^+, C_nH^+, and C_nCN^+ to produce the adducts are quite likely.

Conclusions

The study of HCN reactions with small positive carbon cluster ions has given a number of new and interesting results.

(1) The reactivity of carbon clusters and their HCN reaction products follows a simple empirical rule correlated to the radical/nonradical nature of the ion.

(2) The variations in product branching ratios within a homologous series of reactions can be predicted by energetic considerations alone.

(3) The proposed mechanism for reaction of the linear cluster ions at the carbene sites is only partially correct. The first HCN appears to add covalently at the carbene, but the second HCN preferentially associates with the ion, most likely by hydrogen bonding to the first HCN fragment in the ion.

(4) In addition to C_7^+, the $n = 8$ and 9 clusters are also present as two different structural isomers, which the results indicate are linear and cyclic. There is no compelling evidence for the existence of other cyclic isomers such as C_4^+.

(5) The C_7^+ cluster behaves in an anomalous fashion, which we interpret in part as due to the isomerization of the cyclic form during reaction.

(6) Positive carbon clusters undergo efficient radiative association reactions with HCN. This observation has important implications for interstellar chemistry.

Acknowledgment. We thank V. Anicich (JPL), B. Dunlap, M. Hanratty, and J. Rice for helpful discussions.

Registry No. HCN, 74-90-8.

Fundamental Studies of the Energetics and Dynamics of Ligand Dissociation and Exchange Processes at Transition-Metal Centers in the Gas Phase: $Mn(CO)_x^+$, $x = 1-6$

David V. Dearden,[†] Kathleen Hayashibara,[†] J. L. Beauchamp,*[,†] Nicholas J. Kirchner,[‡] Petra A. M. van Koppen,[‡] and Michael T. Bowers*[,‡]

Contribution No. 7850 from the Arthur Amos Noyes Laboratory of Chemical Physics, California Institute of Technology, Pasadena, California 91125, and Department of Chemistry, University of California, Santa Barbara, California 93106. *Received September 14, 1988*

Abstract: A significant change in spin multiplicity results from sequential addition of CO to Mn^+ (^7S) to form $Mn(CO)_6^+$ ($^1A_{1g}$). To explore the possible effects of changes in spin multiplicity on the dynamics of ligand dissociation and exchange processes at transition-metal centers in the gas phase, we have measured labeled CO exchange rates ($x = 1-6$) and kinetic energy release distributions (KERDs) for metastable decomposition by loss of CO ($x = 2-6$) for $Mn(CO)_x^+$. With the exception of the coordinatively saturated species $Mn(CO)_6^+$, for which no ligand exchange is observed, the CO exchange rates are within an order of magnitude of collision limited in all cases. All KERDS were statistical, indicating no barrier in the CO-loss exit channel. These results are discussed in terms of the requirements for spin conservation in ligand exchange reactions. Quantitative analysis of statistical KERDs requires a knowledge of the internal energy of the decomposing species, which in the present experiment are formed by electron impact with a broad range of internal energies. We demonstrate that the temporal constraints of the experiment select metastables with a particular range of internal energies, which can be bracketed using RRKM theory, enabling the KERDs to be modeled using phase space theory. Individual $D_0^0(Mn(CO)_{x-1}^+-CO)$ (kcal/mol) values were determined by fitting the phase space calculations to the experimental KERDs: $x = 6$, 32 ± 5; $x = 5$, 16 ± 3; $x = 4$, 20 ± 3; $x = 3$, 31 ± 6; $x = 2$, <25; $x = 1$, >7.

In a recent series of studies on the addition rates of CO to coordinatively unsaturated, neutral metal carbonyls, spin conservation was used to explain the large variations in the rates for reaction 1 among members of the $Fe(CO)_x$ system. For $x = 4$,

$$M(CO)_x + CO \rightarrow M(CO)_{x+1} \quad (1)$$

the rate was 2.5 orders of magnitude slower than that for $x = 3$ or $x = 2$, which have rates within 1 order of magnitude of the collision rate.[1,2] Since $Fe(CO)_5$ has a singlet ground state while $Fe(CO)_4$ is known from magnetic circular dichroism studies to be a triplet,[3] the recombination rates were taken to be a reflection of the spin-forbidden nature of CO addition to $Fe(CO)_4$, while it was assumed that CO addition to $Fe(CO)_2$ and to $Fe(CO)_3$ are spin-allowed processes. Subsequent studies on $Cr(CO)_x$ ($x = 5-2$)[4,5] and $Co(CO)_x$ ($x = 1-3$)[6] found that the CO recombination rates were all fast, leading to the suggestion that all of these recombination reactions proceed with spin conservation. A natural question arising from this work is whether or not the spin conservation requirement for rapid reaction is general.

* Authors to whom correspondence should be addressed.
[†] California Institute of Technology.
[‡] University of California.

(1) Ouderkirk, A. J.; Wermer, P.; Schultz, N. L.; Weitz, E. *J. Am. Chem. Soc.* **1983**, *105*, 3354-3355.
(2) Seder, T. A.; Ouderkirk, A. J.; Weitz, E. *J. Chem. Phys.* **1986**, *85*, 1977-1986.
(3) Barton, T. J.; Grinter, R.; Thomson, A. J.; Davies, B.; Poliakoff, M. *J. Chem. Soc., Chem. Commun.* **1977**, 841-842.
(4) (a) Fletcher, T. R.; Rosenfeld, R. N. *J. Am. Chem. Soc.* **1985**, *107*, 2203-2212. (b) Fletcher, T. R.; Rosenfeld, R. N. *J. Am. Chem. Soc.* **1986**, *108*, 1686-1688. (c) Fletcher, T. R.; Rosenfeld, R. N. *J. Am. Chem. Soc.* **1988**, *110*, 2097-2101.
(5) (a) Seder, T. A.; Church, S. P.; Ouderkirk, A. J.; Weitz, E. *J. Am. Chem. Soc.* **1985**, *107*, 1432-1433. (b) Seder, T. A.; Church, S. P.; Weitz, E. *J. Am. Chem. Soc.* **1986**, *108*, 4721-4728.
(6) Rayner, D. M.; Nazran, A. S.; Drouin, M.; Hackett, P. A. *J. Phys. Chem.* **1986**, *90*, 2882-2888.

0002-7863/89/1511-2401$01.50/0